

Application of superconducting-superfluid magnetohydrodynamics to nuclear pasta in neutron stars

D. N. Kobyakov^{1,*}

¹*Institute of Applied Physics of the Russian Academy of Sciences, 603950 Nizhny Novgorod, Russia*

(Dated: December 14, 2024)

Hydrodynamic equations of motion of uniform superconducting and superfluid liquids of protons coupled to ultrarelativistic electron gas, and neutrons are derived from low-energy effective Hamiltonian based on the well defined degrees of freedom: the superfluid densities and phases. The Hamiltonian accounts for relativistic contributions to the nucleon mass densities from strong interactions. Based on this, non-dissipative magneto-hydrodynamic (MHD) equations are derived. The equations feature the well-known Lorentz force for proton superflows, and a magnetic force for neutron superflows, which depends on the magnetic field and the relative superfluid motion, and has not been considered in astrophysical applications. We consider anisotropic superfluid density tensor of the pasta phase, and calculate possible contribution to the elastic stress tensor of the crust from the neutron magnetic force in lasagne phase. We show that magnitude of this force for typical conditions preceding a magnetar flare or a glitch activity (magnetic field $\sim 10^{14}$ G and baryon velocity lag ~ 1 cm s⁻¹) may be significant for global stability of the crust and may lead to crust breaking and subsequent starquakes, if the magnetic field penetrates the superconducting region on a macroscopic length scale $\gtrsim 1$ cm. Analogy with terrestrial superconducting and polycrystalline materials suggests that the latter condition is likely to be satisfied in slabs of nuclear pasta immersed in parallel magnetic field.

Introduction. The MHD in superconducting-superfluid mixtures is crucial for interpretation of many phenomena related to neutron stars [1]. Several works have formulated equations of motion for mixtures of two superfluids with entrainment [2–5, 8]. These works neglected relativistic contributions to the total mass density from strong interactions and from the effective electron mass. The corrections are of the order of $\mu_e/m_\alpha c^2 \sim 10\%$, where μ_e is the electron chemical potential, c is the speed of light and m_α is the rest nucleon mass ($\alpha = p$ for protons and n for neutrons) [9]. The nucleon mass consists of the rest mass and the relativistic contribution from strong interactions,

$$M_\alpha = m_\alpha + \mu_\alpha^{\text{nuc}}/c^2, \quad (1)$$

where $\mu_\alpha^{\text{nuc}} = \partial E_{\text{st}}^{\text{nuc}}/\partial n_\alpha$ are the chemical potentials in the absence of flows and without the rest mass contribution. The static energy density $E_{\text{st}}^{\text{nuc}}(n_p, n_n)$ is calculated from the equation of state of nuclear matter, where n_α are the nucleon number densities in three-dimensional bulk. These corrections will be taken into account in this Letter, and will be collectively called *inertia corrections*.

As a first step, we derive the coupled Josephson equations:

$$\hbar \partial_t \phi_p + \frac{\pi_p^2}{2M_p} - \frac{1}{2} \frac{\partial \rho_{np}}{\partial n_p} \mathbf{w}^2 + r_p = -\tilde{\mu}_p, \quad (2)$$

$$\hbar \partial_t \phi_n + \frac{\pi_n^2}{2M_n} - \frac{1}{2} \frac{\partial \rho_{np}}{\partial n_n} \mathbf{w}^2 + r_n = -\mu_n^{\text{nuc}}, \quad (3)$$

where $\pi_p = \mathbf{p}_p - e\mathbf{A}/c$ is the proton gauge-invariant momentum, e the proton charge, \mathbf{A} is the vector potential, $\mathbf{p}_\alpha = \hbar \nabla \phi_\alpha$ is the *momentum* per nucleon, $2\phi_\alpha$ is the phase of the superfluid order parameter, $\tilde{\mu}_p = e\Phi + \mu_p^{\text{nuc}}$ is the proton chemical potential including energy in the electric potential Φ , and $\mathbf{w} = \pi_p/M_p - \pi_n/M_n$. The relativistic corrections are represented by M_α and r_α , Eq. (13). The nonrelativistic form of these equations, with $M_\alpha \rightarrow m_\alpha$ and $r_\alpha \rightarrow 0$, is well-known in

the context of superfluid mixtures with entrainment [2, 8, 10]. The entrainment mass density is

$$\rho_{np} = (M_p M_n / 9\pi^4) k_{Fn}^2 k_{Fp}^2 f_1^{np}, \quad (4)$$

where f_1^{np} is the Landau parameter and $k_{F\alpha}$ is the nucleon Fermi wavenumber.

Next, we derive the equation of motion of neutron momentum, Eq. (15) and find neglecting the inertia corrections, that there is a magnetic force per neutron,

$$\mathbf{F}_{Ln} = -\frac{e}{m_p c} \frac{\partial \rho_{np}}{\partial n_n} \mathbf{w} \times \mathbf{B}, \quad (5)$$

where $\mathbf{B} = \nabla \times \mathbf{A}$, which has been first discussed in [11]. It is notable that this force is present implicitly in the momentum equations in [2]. This force depends on the superfluid momentum lag \mathbf{w} , and thus is qualitatively different from the macroscopically averaged neutron magnetic force considered in [12], which does not depend on \mathbf{w} . Here, averaging over vortex and fluxtube lattices is not performed, and we do not consider dissipative forces acting on the singularities.

Analogy with terrestrial superconducting materials [13], suggests that the quasi two-dimensional (2D) nuclear matter inside the slabs of the lasagne phase at typical conditions is superconducting and superfluid. The neutron magnetic force, Eq. (5), is astrophysically important if the effective magnetic penetration depth is sufficiently large. This condition may be satisfied in a polycrystalline nuclear pasta in neutron stars.

In an ideal crystalline phase of slabs, the stable equilibrium is expected to be configuration with horizontally oriented slabs with parallel magnetic field originating from the toroidal component, as sketched in Fig. 1 a. The effective penetration depth of the magnetic field in Fig. 1 a is expected to be microscopic; the precise value can be found with the help of a Ginzburg-Landau theory, which is not considered here. However, possible polycrystalline structure of the crust [14] sup-

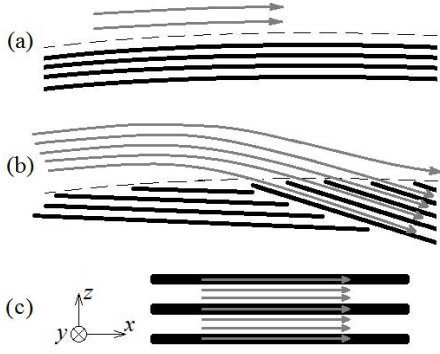


FIG. 1. (Color online) Schematic picture of possible configurations of parallel magnetic field in (a) ideal crystalline and in (b) polycrystalline lasagne phase of nuclear matter in the mantle of neutron stars. (c) Magnified view of a fluid element containing the slabs immersed in parallel magnetic field. Dashed line shows the low-density boundary of the lasagne phase. Thick solid lines show the cross section of the lasagne slabs. The magnetic field lines are displayed by arrows.

ports an assumption that the magnetic field penetrates deep into the lasagne phase, as schematically shows Fig. 1 b.

The total energy and action. In an ideal irrotational fluid, the low-energy excitations can be described with the help of the canonically conjugated variables – the velocity potential (the superfluid phase ϕ_α) and the number density n_α [15]. Using the effective degrees of freedom and neglecting the nuclear surface corrections, we write the total energy of matter:

$$H_{\text{tot}}^{\text{matt}} = E_{\text{st}}^{\text{nuc}}(n_p, n_n) + E_{\text{kin}}^{\text{nuc}}(n_p, n_n, \pi_p, \mathbf{p}_n) + E_{\text{Coul}}^{\text{p}}(n_p, A_0) + E^{\text{e}}(n_e, \mathbf{J}_e, A_0) + E_{\text{Coul}}^{\text{e}}(n_e, \mathbf{J}_e, A_0, \mathbf{A}). \quad (6)$$

The energy density of the ultrarelativistic degenerate electrons is $E^{\text{e}} = \mu_e^4 / 4\pi^2 (\hbar c)^3$, and $\mu_e = \hbar c (3\pi^2 n_e)^{1/3}$ is the electron chemical potential with n_e being the electron number density. Contribution of the electrons in electromagnetic field to the total energy is given by $E_{\text{Coul}}^{\text{e}} = -en_e \Phi - \frac{1}{c} \mathbf{J}_e \cdot \mathbf{A}$, where \mathbf{J}_e is the electronic current [16]. Proton contribution to electromagnetic interactions comes from $E_{\text{Coul}}^{\text{p}} = en_p \Phi$, and from the kinetic energy density. The electromagnetic energy density is given by its standard form, $E^{\text{em}} = (8\pi)^{-1} (E^2 + B^2)$, where $\mathbf{E} = c^{-1} (-\nabla A_0 - \partial_t \mathbf{A})$ is the electric field and $\mathbf{B} = \nabla \times \mathbf{A}$ is the magnetic induction and (A_0, \mathbf{A}) is the electromagnetic four-potential with $A_0 = c\Phi$ [16]. The baryon mass densities carried by excitations are $\rho_\alpha = M_\alpha n_\alpha$. Macroscopic velocities of the nuclear fluids in realistic conditions are nonrelativistic, and therefore the kinetic energy density is a quadratic form of the momenta:

$$E_{\text{kin}}^{\text{nuc}} = \frac{\rho_p \pi_p^2}{2M_p^2} + \frac{\rho_n \mathbf{p}_n^2}{2M_n^2} - \frac{\rho_{np}}{2} \left(\frac{\pi_p}{M_p} - \frac{\mathbf{p}_n}{M_n} \right)^2. \quad (7)$$

The total action S is

$$S = \int d^3 \mathbf{r} (\mathcal{T} - H_{\text{tot}}) + S^{\text{em}}, \quad (8)$$

where $\mathcal{T} = -\hbar n_p \partial_t \phi_p - \hbar n_n \partial_t \phi_n$ and $S^{\text{em}} = (1/16\pi) \int d^3 \mathbf{r} \sum_{a,b=0,1,2,3} (\partial_a A_b - \partial_b A_a)^2$. More generally, hydrodynamics in a mixture of neutral fluids can be formulated in terms of the Lorentz-invariant four-current vector and four-momentum covector [17], and sound speeds can be calculated [18]. However, it would be useful to reveal role of the electrons explicitly, which can be done by the method of response functions used below.

The equations of motion. Equations of motion result from minimization of the action with respect to its functional degrees of freedom. The continuity equations are derived from variations of S with respect to ϕ_α :

$$\partial_t n_\alpha + \nabla \cdot \mathbf{J}_\alpha^{\text{num}} = 0. \quad (9)$$

The velocity of nucleon flows \mathbf{v}_α is $\mathbf{v}_\alpha = \mathbf{J}_\alpha^{\text{num}} / n_\alpha$. The number current is $\mathbf{J}_\alpha^{\text{num}} = \partial E / \partial \mathbf{p}_\alpha = \partial H_{\text{tot}}^{\text{matt}} / \partial \mathbf{p}_\alpha$, where $E = H_{\text{tot}}^{\text{matt}} + E^{\text{em}}$ is the total energy density. It is convenient to introduce matrix of number densities $\eta_{\alpha\beta}$ by rewriting the number currents as $\mathbf{J}_p^{\text{num}} = \eta_{pp} \pi_p + \eta_{np} \mathbf{p}_n$, $\mathbf{J}_n^{\text{num}} = \eta_{nn} \mathbf{p}_n + \eta_{np} \pi_p$:

$$\eta_{\alpha\alpha} = (\rho_\alpha - \rho_{np}) / M_\alpha^2, \quad (10)$$

$$\eta_{np} = \rho_{np} / M_p M_n. \quad (11)$$

Using this matrix, we rewrite the kinetic energy density

$$E_{\text{kin}}^{\text{nuc}}(n_p, n_n, \pi_p, \mathbf{p}_n) = \eta_{pp} \pi_p^2 / 2 + \eta_{nn} \mathbf{p}_n^2 / 2 + \eta_{np} \pi_p \cdot \mathbf{p}_n. \quad (12)$$

in the same form that was used earlier [see, for instance, Ref. [19], equation (32)].

Equations for the superfluid phases (the Josephson equations) are obtained from variations of S with respect to n_α , and are given in Eqs. (2) and (3). The relativistic corrections are of order of v_\pm^2 / c^2 and are given by

$$r_p = -\frac{n_p E_{pp}^{\text{nuc}}}{2M_p c^2} \frac{\pi_p^2}{2M_p}, \quad r_n = -\frac{n_n E_{nn}}{2M_n c^2} \frac{\mathbf{p}_n^2}{2M_n}. \quad (13)$$

Smaller corrections of order of $p_n^2 / M_n^2 c^2$ and $\pi_p^2 / M_p^2 c^2$ are neglected, which is consistent with the initial assumption that the flows are nonrelativistic, Eq. (7). The MHD equations for momenta are obtained by application of ∇ to both sides of Eqs. (2) and (3), for example:

$$\partial_t \mathbf{p}_n + \left(\frac{\mathbf{p}_n}{M_n} \cdot \nabla \right) \mathbf{p}_n + \frac{\mathbf{p}_n}{M_n} \times (\nabla \times \mathbf{p}_n) - \frac{\partial \rho_{np}}{\partial n_n} (\mathbf{w} \cdot \nabla) \mathbf{w} - \frac{\partial \rho_{np}}{\partial n_n} \mathbf{w} \times (\nabla \times \mathbf{w}) - \frac{\mathbf{w}^2}{2} \nabla \frac{\partial \rho_{np}}{\partial n_n} + \mathbf{R}_n = -\nabla \mu_n^{\text{nuc}}, \quad (14)$$

where $\mathbf{R}_n = -(\nabla \mu_n^{\text{nuc}} / 2M_n^2 c^2) p_n^2 + \nabla r_n$. To reveal forces given in Eq. (14), which determine the flow properties of neutrons we extract the material derivative $\frac{\partial}{\partial t} + \mathbf{v}_n \cdot \nabla$, and consider the limit $M_\alpha \rightarrow m_p$. By definition, the neutron velocity is $\mathbf{v}_n = m_p^{-1} [\mathbf{p}_n - \frac{\rho_{np}}{\rho_n} (\mathbf{p}_n - \pi_p)]$, however the first and fourth terms in Eq. (14) provide the expression $\frac{\partial}{\partial t} \mathbf{p}_n + m_p^{-1} [\mathbf{p}_n - \frac{\partial \rho_{np}}{\partial n_n} (\mathbf{p}_n - \pi_p)] \cdot \nabla \mathbf{p}_n$. Using results of the previous studies [9]

we assume that the condition $\partial \rho_{np}/\partial n_\alpha = \rho_{np}/n_\alpha$ holds in nuclear matter and find

$$\left(\frac{\partial}{\partial t} + \mathbf{v}_n \cdot \nabla\right) \mathbf{p}_n = -\frac{e}{m_p c} \frac{\rho_{np}}{n_n} \mathbf{w} \times \mathbf{B} - \nabla \mu_n^{\text{nuc}}. \quad (15)$$

The right-hand side of Eq. (15) represents a (nondissipative) force per neutron. The proton momentum equation is

$$\left(\frac{\partial}{\partial t} + \mathbf{v}_p \cdot \nabla\right) \pi_p = e(\mathbf{E} + \frac{1}{c} \mathbf{v}_p \times \mathbf{B}) - \nabla \mu_p^{\text{nuc}}, \quad (16)$$

which contains the Ampère force, two first terms in the right-hand side. The terms $[\nabla(\partial \rho_{np}/\partial n_n)] \mathbf{w}^2$ and $m_p^{-1}(\rho_{np}/n_n)(\mathbf{w} \cdot \nabla) \pi_p$ have been neglected in Eq. (15), and the terms $[\nabla(\partial \rho_{np}/\partial n_p)] \mathbf{w}^2$ and $m_p^{-1}(\rho_{np}/n_p)(\mathbf{w} \cdot \nabla) p_n$ have been neglected in Eq. (16). Dynamics of magnetic field in fluxtubes of proton type-II superconductor may be described by the thermodynamics [3, 5–7]. Below, we focus on neutron flows.

Variation of S with respect to the four-vector potential (A_0, \mathbf{A}) leads to Maxwell equations [16]

$$\nabla \times (\nabla \times \mathbf{A}) - \frac{1}{c} \partial_t \mathbf{E} = \frac{4\pi}{c} \mathbf{J}_{\text{tot}}, \quad (17)$$

$$\nabla \cdot \mathbf{E} = 4\pi e(n_p - n_e), \quad (18)$$

where $\mathbf{J}_{\text{tot}} = \mathbf{J}_s + \mathbf{J}_e$ is the total electric current. The superfluid contribution to \mathbf{J}_{tot} is given by $\mathbf{J}_s = e \mathbf{J}_p^{\text{num}}$. Using the Coulomb gauge for the vector potential, $\nabla \cdot \mathbf{A} = 0$, from Eq. (18) one obtains the Poisson equation

$$\nabla^2 \Phi = -4\pi e(n_p - n_e). \quad (19)$$

Linear hydrodynamic modes. In order to quantitatively understand the role of the relativistic inertia corrections for the physical properties, we consider the linear modes with zero background velocities of nucleons. Here, the electrons are in the hydrodynamic regime and the damping rate of the modes is negligible. Linearizing the right-hand sides of Eqs. (2) and (3), we obtain

$$\delta \tilde{\mu}_p = E_{np} \delta n_n + \left(E_{pp}^{\text{nuc}} + \frac{4\pi e^2}{k^2} \frac{1}{\epsilon_e(\omega, k)}\right) \delta n_p, \quad (20)$$

$$\delta \mu_n^{\text{nuc}} = E_{nn} \delta n_n + E_{np} \delta n_p, \quad (21)$$

where $E_{pp}^{\text{nuc}} = \partial^2 E^{\text{nuc}}/\partial n_p^2$, $E_{nn} = \partial^2 E^{\text{nuc}}/\partial n_n^2$, $E_{np} = \partial^2 E^{\text{nuc}}/\partial n_p \partial n_n$, and $\epsilon_e(\omega, k) = 1 + (4\pi e^2/k^2) \chi_0(\omega, k)$ is the dielectric function of the electrons. It is convenient to introduce the quantity $E_{pp} = E_{pp}^{\text{nuc}} + 4\pi e^2/k^2 \epsilon_e(\omega, k)$. In the hydrodynamic regime, the response function $\chi_0(\omega, k)$ has the form

$$\chi_0(\omega, k) = \frac{\partial n_e}{\partial \mu_e} \frac{c_e^2 k^2}{c_e^2 k^2 - \omega^2}, \quad (22)$$

where $c_e = c/\sqrt{3}$ [9]. Using Eq. (22), we obtain from Eq. (20)

$$\delta \tilde{\mu}_p = -E_{np} \delta n_n - \left[E_{pp}^{\text{nuc}} + \frac{\partial \mu_e}{\partial n_e} \left(1 - \frac{v^2}{c_e^2}\right)\right] \delta n_p. \quad (23)$$

Linear hydrodynamic modes $\propto \exp(-i\omega t + ikx)$ with $v \equiv \omega/k$ are obtained by setting the vector potential to zero, $\mathbf{A} = 0$, and linearizing Eqs. (2), (3) and (9):

$$\begin{pmatrix} -v & 0 & \eta_{pp} & \eta_{np} \\ 0 & -v & \eta_{np} & \eta_{nn} \\ E_{pp} & E_{np} & -v & 0 \\ E_{np} & E_{nn} & 0 & -v \end{pmatrix} \begin{pmatrix} \delta n_p \\ \delta n_n \\ \delta p_p \\ \delta p_n \end{pmatrix} = 0. \quad (24)$$

The thermodynamic derivative E_{pp} consists of a contribution due to the electron and proton compressibility, which is denoted $E_{pp}^{\text{st}} = E_{pp}^{\text{nuc}} + \partial \mu_e / \partial n_e$, and due to the electron effective mass, $-(\partial \mu_e / \partial n_e)(v^2/c_e^2)$. Equation (24) reduces to

$$v^4 (1 + \eta_{pp} \tilde{\mu}'_e) - (B^{\text{st}} + \tilde{B}) v^2 + C^{\text{st}} = 0, \quad (25)$$

where $\tilde{\mu}'_e \equiv c_e^{-2} \partial \mu_e / \partial n_e$, and the coefficients are

$$B^{\text{st}} = \eta_{nn} E_{nn} + 2\eta_{np} E_{np} + \eta_{pp} E_{pp}^{\text{st}}, \quad (26)$$

$$\tilde{B} = \tilde{\mu}'_e E_{nn} \det \eta_{\alpha\beta}, \quad (27)$$

$$C^{\text{st}} = \det \eta_{\alpha\beta} \det E_{\alpha\beta}^{\text{st}}, \quad (28)$$

where $\det \eta_{\alpha\beta} = \eta_{pp} \eta_{nn} - \eta_{np}^2$ and $\det E_{\alpha\beta}^{\text{st}} = E_{pp}^{\text{st}} E_{nn} - E_{np}^2$. The uncoupled mode speeds $v_{\alpha 0}^{\text{in}}$ are obtained by setting $E_{np} = 0$ and $\eta_{np} = 0$ in Eq. (24):

$$(v_{p0}^{\text{in}})^2 = \frac{1}{M_p^{\text{eff}}} n_p E_{pp}^{\text{st}}, \quad (v_{n0}^{\text{in}})^2 = \frac{1}{M_n} n_n E_{nn}, \quad (29)$$

where $M_p^{\text{eff}} = M_p + \mu_e/c^2$. The eigenmodes given in Eqs. (24) and (25) can be compared with the earlier work. The linearized matrix in Eq. (24) accounts for the inertia corrections and reduces to the case of a mixture of two neutral superfluids at zero temperature [8], when the following approximations are made: $\chi_0(\omega, k) \rightarrow \chi_0^{\text{st}} = \partial n_e / \partial \mu_e$, $M_\alpha \rightarrow m_\alpha$, and $m_\alpha \rightarrow m_p \equiv m$. It is notable that the approximation $\chi_0(\omega, k) \rightarrow \chi_0^{\text{st}}$ leads to disappearance from M_p^{eff} of the electron contribution, $M_p^{\text{eff}} \rightarrow M_p$. The eigenmode velocities were also studied earlier within a model limited by the condition of beta-equilibrium $\delta \mu = 0$, where $\delta \mu = (M_p^{\text{eff}} - M_n) c^2$ (see [19] and Ref. 21 therein). In that model, the eigenmode equation was found and can be written in the notation of this Letter: $v^4 (1 + \eta_{pp} \tilde{\mu}'_e) - b v^2 + C^{\text{st}} = 0$, with $b = (B^{\text{st}} + \tilde{B}) - E_{nn} \det[\eta_{\alpha\beta}] \delta \mu / n_p c^2$ [20]. That result, derived by a rather different method coincides with Eq. (25), when $\delta \mu = 0$. It is notable that the approach used here is free of the condition $\delta \mu = 0$, as long as the source terms in the baryon continuity equations can be neglected. This neglect is an excellent approximation on hydrodynamic time scales for sufficiently cold matter even when $\delta \mu \neq 0$ [1].

Numerical results: chemical potentials and linear modes. As a first step, we calculate μ_α^{nuc} and μ_e at beta equilibrium using the effective chiral field theory [21]. The results are shown in Table I. Other basic parameters of the model, $E_{\alpha\beta}$ and η_{np} , are given in [9]. For the entrainment parameter we use $\eta_{np} = -3.125 \text{ fm}^3 n_p n_n m_p^{-1}$ [9]. The collective mode velocities are calculated using Eq. (25). The left panel of Fig.

$n(\text{fm}^{-3})$	$n_p(\text{fm}^{-3})$	μ_e (MeV)	μ_p^{nucl} (MeV)	μ_n (MeV)
0.08	2.64×10^{-2}	84.37	-69.05	14.11
0.16	7.746×10^{-3}	120.8	-90.15	29.32
0.24	1.236×10^{-2}	141.1	-87.85	51.87
0.32	1.513×10^{-2}	151.0	-69.15	80.43

TABLE I. The total baryon density, beta-equilibrium proton density, the electron chemical potential, the nuclear interaction contributions to the chemical potentials, calculated from the effective chiral field theory [21].

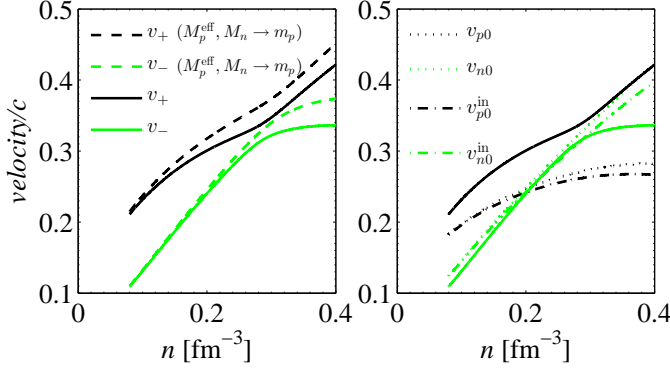


FIG. 2. (Color online) *Left panel.* Velocities of the coupled eigenmodes v_{\pm} , Eq. (25), with inertia corrections (solid lines), and neglecting these corrections (dashed lines). *Right panel.* Coupled eigenmodes v_{\pm} , uncoupled eigenmodes with inertia corrections $v_{\alpha 0}^{\text{in}}$, Eqs. (29), and the uncoupled modes neglecting these corrections $v_{\alpha 0}$.

2 shows that the mode speeds are lowered by the inertia corrections, as expected from general considerations. The effect is small, which confirms its neglect in earlier work [8]. The right panel of Fig. 2 compares effects of the inertia corrections with the effect of mode coupling due to E_{np} and ρ_{np} , and shows that the coupling affects the mode speeds significantly stronger than do the inertia corrections.

Astrophysical applications. As a first application, we find the magnetic flux quantum κ_{α} associated with a proton and a neutron phase singularity (phase winding around the singularity line in 3D, or point in 2D, is 2π). Using the standard considerations, we obtain $\kappa_p = \pi\hbar c/e$ and $\kappa_n = (\eta_{np}/\eta_{pp})\pi\hbar c/e$. It is interesting to note that κ_p is not affected by the inertia corrections, while κ_n is reduced as much as by about 10% compared with the standard value Φ_* [22]. The effect of inertia corrections on the magnetic field penetration depth $\Lambda_{*in}^2 = c^2/4\pi e^2\eta_{pp}$ is to decrease its value by about 5%.

Next, we consider a large number of parallel thin slabs immersed in a parallel magnetic field, as schematically shows Fig. 1 c. In uniform nuclear matter, the coherence length ~ 30 fm and the London penetration depth ~ 80 fm [22]. Typical slab width is ~ 4 fm and separation is ~ 10 fm [23]. Since the slab thickness is much smaller than the London penetration depth, the magnetic field completely penetrates into the slab and can be assumed uniform, as schematically shows Fig. 1

c. Length of the slabs is limited by the Landau-Pierls instability [24]. The lattice of slabs extends into some depth d along z axis. The total macroscopic force $F_{Ln}^{1\text{cm}^2 \times d}$ acting on superfluid neutrons inside the lasagne slabs in a volume $1\text{cm}^2 \times d$ is given by the volume integral of the force density per neutron multiplied by the superfluid neutron number density. In the pasta phase, the superfluid densities of protons and neutrons are tensors with anisotropic properties. Motion of protons perpendicularly to the slab surface is not superfluid (tunnelling between the slabs is neglected) being a result of the Coulomb crystal deformations and motion of the center of mass of the lattice element, analogously to the situation in the inner crust [25], and here it is irrelevant. The parallel component of the superfluid density tensor is simply the saturation number density of the corresponding nucleon species multiplied by the volume fraction of the pasta phase in the unit cell.

We consider superfluid motion inside the slab, with \mathbf{w} parallel to the slab surface ($x-y$ plane). The angle between \mathbf{B} and \mathbf{w} is θ . The right-hand side of Eq. (15) is nonzero due to the second term, which provides a neutron magnetic force along z axis, $(\mathbf{F}_{Ln})_z$. By virtue of continuity of stress, this force exerts an external elastic stress on the crust, σ_{ij}^{ex} . Before a starquake, the fluid element shown in Fig. 1 c is in equilibrium and does not move along z . The force balance in the solid crust reads:

$$0 = -p\delta_{ij} + \sigma_{ij}^{\text{ex}} + \mu u_{ij} + M_{ij}, \quad (30)$$

where p is pressure, μ_{eff} is the effective shear modulus of polycrystalline solid, u_{ij} is the strain tensor, and M_{ij} is the Maxwell stress tensor. We assume density inside the slab is 0.16 fm^{-3} and that the superfluid neutron density can be represented by Heaviside step functions, and thus $\rho_{np}/n_n \equiv g_0 \sim -0.0242m_p$ [9]. Therefore, there are 6.4×10^{25} neutrons inside a single slab with surface 1 cm^2 and width 4 fm. If distance between centers of the slabs is 10 fm, a simple calculation shows that there are $N_n = 6.4 \times 10^{37} \frac{d}{1\text{cm}}$ superfluid neutrons in a superconducting-superfluid mixture, in a $1\text{cm}^2 \times d\text{cm}$ column of the lasagne matter. The velocity lag $\mathbf{v}_p - \mathbf{v}_n$, which in typical conditions assumed to be $\sim 1 \text{ cm}$, is related to \mathbf{w} [8]: $\mathbf{v}_p - \mathbf{v}_n = (n_p n_n)^{-1} (\det m_p \eta_{\alpha\beta}) \mathbf{w}$, and one finds $\mathbf{v}_p - \mathbf{v}_n = 0.9884 \mathbf{w}$. The total neutron magnetic force acting on a $1\text{cm}^2 \times d$ column of lasagne immersed in a uniform magnetic field is

$$\begin{aligned} \left(\mathbf{F}_{Ln}^{1\text{cm}^2 \times d} \right)_z &\sim N_n \frac{e}{m_p c} |g_0| w B = 2.511 \times 10^{30} \\ &\times \left(\frac{d}{1\text{cm}} \right) \left(\frac{w}{1\text{cm s}^{-1}} \right) \left(\frac{B}{10^{14}\text{G}} \right) \sin \theta \text{ [dyn]}, \end{aligned} \quad (31)$$

where d is the macroscopic penetration depth of the magnetic field along z , Fig. 1 c. The induced stress is $\sigma_{zz}^{\text{ex}} = \mathbf{F}_{Ln}^{1\text{cm}^2 \times d} \cdot \hat{\mathbf{z}} = \left(\mathbf{F}_{Ln}^{1\text{cm}^2 \times d} \right)_z$. In the present model, the extra stress is balanced by the crust rigidity, while the Maxwell stress tensor does not deform the crust:

$$\mu_{\text{eff}} u_{ij} = \left(\mathbf{F}_{Ln}^{1\text{cm}^2 \times d} \right)_z \quad (32)$$

The latter assumption is in agreement with the prediction of [7] that the crust breaking, with the critical strain $u_{max} \sim 0.1$, occurs at 2.4×10^{15} G which is significantly higher than the typical field 10^{14} G considered here. The crust yielding occurs when von Mises criterion is satisfied [7], $\sqrt{u_{ij}u_{ij}}/2 \geq u_{max}$. For the shear modulus of polycrystalline matter of the inner crust with spherical ions, $\mu_{eff} = 0.3778 \frac{n_N Z^2 e^2}{2a}$ [14], we use the parameters at the bottom of the inner crust, where the ions are spherical at baryon density 7.943×10^{-2} [26]: $n_N = 1.750 \times 10^{-4} \text{ fm}^{-3}$, $Z = 17.23$, $a = (3/4\pi n_N)^{1/3} = 11.09 \text{ fm}$, and find that the crust yields when

$$\frac{\left(\mathbf{F}_{Ln}^{1\text{cm}^2 \times d}\right)_z}{2.040 \times 10^{30} \text{ dyn}} \geq \sqrt{2} u_{max}. \quad (33)$$

Molecular dynamics simulations [27] show that in the neutron star crust $u_{max} \sim 0.1$. Typical neutron magnetic force estimated in Eq. (31), is more than 8 times larger than the critical stress that breaks the crust, which constrains possible values of d , \mathbf{w} and \mathbf{B} .

The precise x-ray burst mechanism in magnetars is an open question [28, 29]. An important problem for future study is characterization of the polycrystalline structure of the crust and its links to the x-ray observations, in particular, determination of basic properties of the polycrystalline phases, sizes of the crystalline domains, effective elasticity, effective electric conductivity, interaction between the magnetic field and the pasta phases.

Acknowledgments. This work was supported by the Russian Fund for Basic Research grant 31 16-32-60023/15. The hospitality of the Ioffe Physical Technical Institute in Saint Petersburg is gratefully acknowledged.

* dmitry.kobyakov@appl.sci-nnov.ru

[1] I. Easson and C. J. Pethick, *ApJ* **227**, 995 (1979).

[2] G. Mendell, *ApJ*, **380**, 515 (1991).

[3] G. Mendell, *MNRAS* **296**, 903 (1998).

[4] R. Prix, *Phys. Rev. D*, **69**, 043001 (2004).

[5] K. Glampedakis, N. Andersson and L. Samuelsson, *MNRAS* **410**, 805 (2011).

[6] I. Easson and C. J. Pethick, *Phys. Rev. D* **16**, 275 (1977).

[7] S. K. Lander, N. Andersson, D. Antonopoulou and A. L. Watts, *MNRAS* **449**, 2047 (2015).

[8] D. N. Kobyakov and C. J. Pethick, *ApJ* **836**, 203 (2017).

[9] D. N. Kobyakov, C. J. Pethick, S. Reddy and A. Schwenk, *Phys. Rev. C* **96**, 025805 (2017).

[10] J. Nespolo, G. E. Astrakharchik and A. Recati, 2017, arXiv:1708.03141.

[11] D. Kobyakov, L. Samuelsson, M. Marklund, E. Lundh, V. Bychkov, & A. Brandenburg, 2015, arXiv:1504.00570v4.

[12] K. Palapanidis, N. Stergioulas and S. K. Lander, *MNRAS* **452**, 3246 (2015).

[13] M. Tinkham, *Phys. Rev.* **129**, 2413 (1963)

[14] D. Kobyakov and C. J. Pethick, *MNRAS Lett.* **449**, L110L112 (2015).

[15] E. M. Lifshitz, and L. P. Pitaevskii, *Statistical Physics, Part 2: Theory of the Condensed State*, (Butterworth-Heinemann, 1980).

[16] L. D. Landau and E. M. Lifshitz, *The Classical Theory of Fields (Volume 2 in Course of Theoretical Physics)*, (Pergamon Press, 1971).

[17] B. Carter and I. M. Khalatnikov, *Phys. Rev. D* **45**, 4536 (1992).

[18] A. Haber, A. Schmitt and S. Stetina, *Phys. Rev. D* **93**, 025011 (2016).

[19] M. E. Gusakov, E. M. Kantor and P. Haensel, *Phys. Rev. C*, **79**, 055806 (2009).

[20] The model used in [19] provides the sound speeds in terms of various thermodynamic derivatives, $\partial/\partial n$ at fixed n_e and $\partial/\partial n$, at fixed x with $x = n_p/n$. Those sound speeds may be rewritten in terms of $E_{\alpha\beta}$ using the relations $\partial/\partial n|_{n_e} = \partial/\partial n_n$ and $\partial/\partial n|_x = (1-x)\partial/\partial n_n + x\partial/\partial n_p$, and the fact that the quantities $Y_{\alpha\beta}$ from [19] are equal to $\eta_{\alpha\beta}$.

[21] K. Hebeler, J. M. Lattimer, C. J. Pethick and A. Schwenk, *ApJ*, **773**, 11 (2013).

[22] M. A. Alpar, S. A. Langer and J. A. Sauls, *ApJ*, **282**, 533 (1984).

[23] G. Watanabe, K. Iida and K. Sato, *Nucl. Phys. A* **676**, 455 (2000).

[24] C. J. Pethick and A. Y. Potekhin, *Phys. Lett. B* **427**, 7 (1998).

[25] D. Kobyakov and C. J. Pethick, *Phys. Rev. C* **87**, 055803 (2013).

[26] D. Kobyakov and C. J. Pethick, *Phys. Rev. C* **94**, 055806 (2016).

[27] C. J. Horowitz and K. Kadau, *Phys. Rev. Lett.* **102**, 191102 (2009).

[28] R. Turolla, S. Zane and A. L. Watts, *Rep. Prog. Phys.* **78**, 116901 (2015).

[29] V. M. Kaspi and A. M. Beloborodov, *Ann. Rev. Astron. Astrophys.* **55**, 261 (2017).